Coordinated Adaptive Cruise Control System With Lane-Change Assistance

Ruina Dang, Jianqiang Wang, Shengbo Eben Li, and Keqiang Li

***Abstract*—To address the problem caused by a conventional adaptive cruise control (ACC) system, which hinders drivers from changing lanes, in this study we propose a novel coordinated ACC system with a lane-change assistance function, which enables dual-target tracking, safe lane change, and longitudinal ride comfort. We first analyze lane-change risk by calculating minimum safety spacing between the host vehicle and surrounding vehicles and then develop a coordinated control algorithm using model predictive control theory. Tracking performance is designed on the basis of tracking errors of the host car and two leading vehicles, safety performance is realized by considering the safe distance between the host car and surrounding vehicles, and ride comfort performance is realized by limiting the vehicle's longitudinal acceleration. Driver-in-the-loop tests performed on a driving simulator confirm that the proposed ACC system can overcome the disadvantages of conventional ACC and achieves multiobjective coordination in the lane-change process.**

***Index Terms*—Adaptive cruise control (ACC), lane-change assistance, minimum safety space, model predictive control (MPC).**

I. Introduction

ADAPTIVE cruise control (ACC) systems, which can improve vehicle safety, smoothen traffic flow, and reduce a driver's workload, have attracted significant attention from various research institutes and automotive companies [1]. The technical development of ACC systems has gradually matured, and it is mainly reflected in multiobjective optimization [2], curve tracking [3], and application to new energy-saving vehicles [4]. However, conventional ACC may hinder the driver from changing lanes, increase the driver's intervention frequency, and reduce its applicability. According to Bosch, whenever the host vehicle approaches a leading vehicle in the same driving lane, the system would decrease the vehicle speed and try to follow the leading vehicle that is in the same lane. If there was an intent to change lanes during this approach, the driver may have to turn off ACC to avoid unexpected deceleration and may have to accelerate to change lanes more quickly and safely [5].

This is not a new issue; it has been studied for many years, particularly in the automotive industry. Rudin-Brown and Parker reported that since ACC shifted the driver's attention from longitudinal operation to lateral control, driver behavior with ACC on was different from that when ACC was off. The difference was mainly reflected in the car-following speed, safety distance when merging, lateral control, and other behaviors [6]. Furthermore, Freyer *et al.* conducted field experiments, comparing driver behavior both with and without ACC switched on. The results showed that ACC increased the frequency of lane-change behaviors for large intervehicle distances. One explanation was that when driving without ACC switched on, the driver's usual lane-change intervehicle distance is short, and the driver tends to slightly accelerate before changing lanes. However, when driving with ACC on, once the intervehicle state fell within the work range of ACC, ACC would reduce the speed of the host vehicle and force it to follow the leading vehicle in the same lane. This deceleration would introduce disturbances to the driver's usual lane-change behavior, and lane changes would be required in advance. They proposed automatic lane change to solve this problem and also designed the controller [7]. Kim *et al.* proposed an ACC and collision avoidance (CA) system with lane-change support, which mainly consisted of a driving decision system, an adaptive cruise controller with an emergency brake function, and a steering controller with lane-change support. They extended the driving choices under special situations and improved the system's safety by adding an automatic lane-change function [8].

However, automatic lane changes may not be the ideal solution to address the problem discussed. On one hand, automatic lane change only completes the longitudinal and lateral movements of the host vehicle while ignoring intervehicle relationships between the host vehicle and surrounding vehicles. On the other hand, except for the throttle and brake pedal, automated lane change also requires that the steering wheel be controlled, which is beyond ACC's control range, and the differences in operation of the two systems may confuse the driver. Moreover, the automatic controller designed in [7] and [8] assumed that the lateral trajectory was similar to sine wave or trapezium, and the longitudinal speed was constant. They ignored the longitudinal change, but this could not satisfy the real driving environment.

To realize the lane-change assistance function, ACC should assess lane-change risk by first checking surrounding vehicles and then controlling the host vehicle to complete lane change in

Manuscript received March 10, 2014; revised July 15, 2014 and October 16, 2014; accepted December 28, 2014. Date of publication February 6, 2015; date of current version September 25, 2015. This work was supported by the National Natural Science Foundation of China under Grant 51205228 and Grant 51175290. The Associate Editor for this paper was H. Jula.

R. Dang is with State Key Laboratory of Automotive Safety and Energy, Tsinghua University, Beijing 100084, China, and also with China North Vehicle Research Institute, Beijing 100072, China (e-mail: drn04@mails.tsinghua.edu.cn).

J. Wang, S. E. Li, and K. Li are with the State Key Laboratory of Automotive Safety and Energy, Tsinghua University, Beijing 100084, China (e-mail: likq@tsinghua.edu.cn).

Color versions of one or more of the figures in this paper are available online at http://ieeexplore.ieee.org.

Digital Object Identifier 10.1109/TITS.2015.2389527

the longitudinal direction if no risk exists. In the assist process, ACC should solve the problem of dual-target tracking between the host vehicle and two leading vehicles in both the same lane and the destination lane, realize multivehicle safety driving performance, and consider the driver's longitudinal comfort requirements.

Model predictive control (MPC) is effective in solving the problem of multiobjective coordination, and it has been widely used in research on vehicle automation. Bageshwar *et al.* designed mode-switching ACC using MPC, which shifted controllers between two modes, i.e., speed control and distance control. The cost function was built using the distance error and relative speed, and the constraint was realized by limiting longitudinal acceleration [9]. Corona and Schutter proposed a hybrid model predictive controller for ACC systems. Longitudinal ride comfort and tracking safety were realized by limiting longitudinal acceleration and minimum distance [10]. Li *et al.* developed a predictive multiobjective controller and employed a constraint-softening method to avoid computational infeasibility. The problem of balance tracking capability, fuel economy, and longitudinal ride comfort is addressed by properly designing the cost function and constraints [11]. Mukai and Kawabe used MPC to realize decision-making for the optimal lane-change trajectory, in which the control objects comprised four aspects: 1) to limit longitudinal acceleration; 2) to reduce lane-change frequency; 3) to approach the driver's desired speed; and 4) to guarantee a suitable time headway (THW) and time to collision (TTC) [12]. Yoshida *et al.* controlled a vehicle's steering through MPC after assuming that the longitudinal speed remained constant during the lane-change process and the steer angle changed like a sine wave. The tire dynamic analysis results demonstrated that lane change had more advantages than an emergency brake [13]. Falcone *et al.* achieved steering control by using MPC to develop an automatic driving vehicle, and system inputs were the steering angle of the front wheel and the slip rates of the four wheels [14]. Brake control was also added to the vehicle to maintain stability during the steering and braking processes [15].

MPC also has great robustness to model uncertainties, and there are many literatures focused on this. Limon, Mayne, and Scokaert pointed out that using robust MPC could guarantee constraint satisfaction and stability of the uncertain system [16]–[18]. Lovett improved MPC robustness in industrial application with statistical process monitoring [19]. Falugi and Mayne converted the problem of obtaining robustness against unstructured uncertainty to the easier problem of achieving robustness against an additional bounded output constraint [20]. Li and Shi investigated the robust distributed MPC problem for a group of nonlinear subsystems subject to control input constraints and external disturbances [21]. If the ACC controller is designed with MPC, the robustness to model uncertainties will be ensured.

As described above, the existing literatures proposed that the ACC hindered lane-change behavior and tried to solve the problem with automatic lane change, which could not satisfy the real driving condition indeed. This study takes the lead to propose a novel ACC with a lane-change assistance function (LCACC), it completes the lane-change behavior with the coordination of the driver. The former controls the longitudinal movement, whereas the latter operates the steering wheel to complete the lateral movement. When assisting the longitudinal motion, the controller takes the two leading vehicles as a virtual one and ensures the "smoothly switch" between the two leading vehicles by designing a fuzzy logic conditioning system. In particular, the system first assesses lane-change risk and then assists the lane-change vehicle to finish the longitudinal movement if no risk exists. The controller is designed with MPC theory, reaching the multiobjective coordination of dual-target tracking, safety lane change, and longitudinal ride comfort. The remainder of this paper is organized as follows. Section II introduces the system structure of LCACC. Section III describes the lane-change warning method considering intervehicle kinetic dynamics. Section IV uses MPC to design its controller, including plant dynamics modeling, performance index design, and optimization problem formulation. Section V illustrates its success using a driver-in-the-loop experiment. Section VI concludes this paper.

II. System Structure

Fig. 1 shows the structure of the proposed LCACC system, including blocks for state detection, lane-change warning, ACC, and vehicle dynamics. The detected states include the host vehicle H and the surrounding vehicles, which are the leading vehicle in the originating lane L_o, the leading vehicle in the destination lane L_d, the rear vehicle in the originating lane R_o, and the rear vehicle in the destination lane R_d. The lane-change warning algorithm first calculates minimum safety spacing (MSS) between H and each surrounding vehicle and then assesses lane-change risk. The ACC outputs the desired longitudinal acceleration after choosing one mode among the three control modes, i.e., cruise control (CC), conventional ACC (ACC), and LCACC. The inverse longitudinal dynamic model transfers the desired longitudinal acceleration $a_{x\,\mathrm{des}}$ to the desired throttle angle $(a_{\mathrm{th\,des}})$ or brake pressure $(P_{B\mathrm{des}})$. The vehicle model responds to the former's output and realizes longitudinal dynamic movement.

As described above, the LCACC system has three control modes. When lane-change intent is detected, the system first analyzes lane-change risk. If no risk exists, the system will switch to the LCACC mode and handover to the other two modes after lane change is complete. On the contrary, the warning signal will switch on, and the system will keep following the vehicle L_o.

In the LCACC control process, if the intervehicle state between H and L_d is beyond the ACC's work range (i.e., the lane-change space is sufficient in the destination lane), the algorithm will directly switch to CC. Otherwise, it needs to solve the multiobjective coordination optimization problem of dual-target tracking, multivehicle safety driving, and longitudinal ride comfort.

This study aims to design multiobjective coordination LCACC. The ACC controller modifies the car-following weight coefficients between H and the two leading vehicles (λ_{lo} and λ_{ld}), predicts the future movements of H and the four surrounding vehicles in the prediction horizon, constructs the

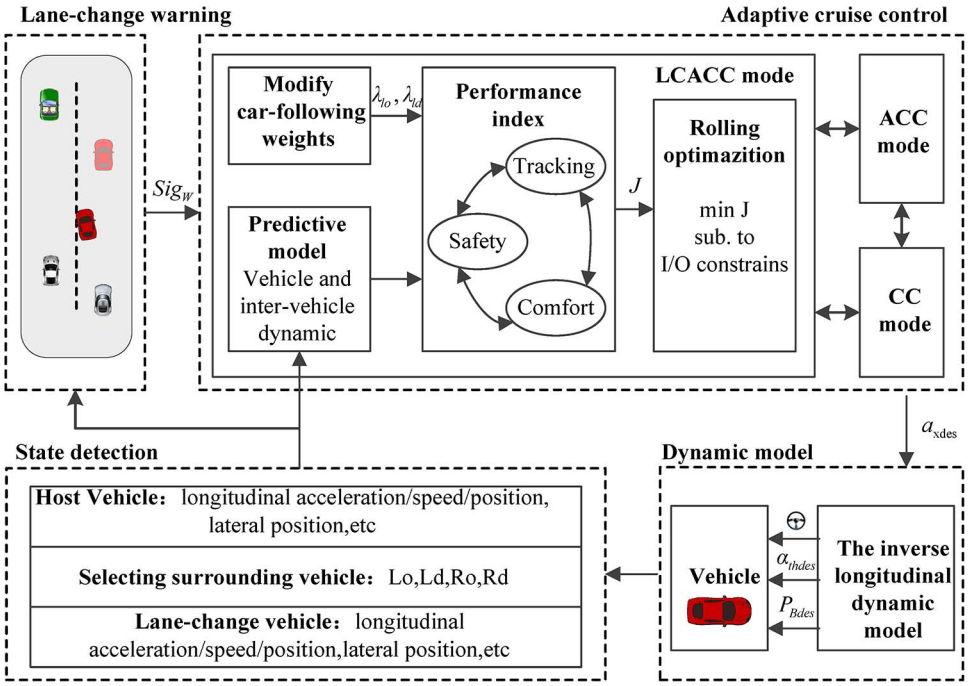

Fig. 1. LCACC system structure.

comprehensive performance index coordinating tracking, safety and comfort, solves the optimization problem, and outputs the desired acceleration.

III. Lane-Change Warning Algorithm

To realize successful lane changes, it is important to ensure a safe intervehicle distance. Therefore, it is necessary to assess lane-change risk by designing a suitable lane-change warning algorithm. The core of the lane-change warning algorithm is to design a reasonable MSS. This section analyzes the MSS between H and each surrounding vehicle from various perspectives. If none of the real intervehicle distances are smaller than the calculated MSS, the lane change is safe.

The MSS between H and R_d is designed for avoiding collisions and maintaining following. The assumption is as follows: If the speed of vehicle R_d is larger than the speed of vehicle H, or similar to it, the collision risk might be higher. Assuming that the speed of vehicle H is constant during the lane-change process, and it is slower than the beginning speed of R_d. After a certain reaction time, the driver in R_d recognizes the lane-change intent of H and brakes to maintain a safe intervehicle distance. When the speed of R_d is equal to the speed of H, the intervehicle distance reaches a minimum value, and this distance should at least be equal to the safe car-following distance. While, if the speed of vehicle R_d is obviously smaller, the collision risk might be lower, and the MSS is designed to be the safe car-following distance. Here, "obviously smaller" is defined as that the speed difference is larger than 5 km/h.

The MSS between H and L_d is designed to prevent the occurrence of collisions. Assuming that L_d brakes with a maximum acceleration and H brakes with the same acceleration after a certain reaction time, the intervehicle distance between the two vehicles should be larger than 0 m when both of them stop.

The MSS between H and the other two vehicles is designed on the basis of safe car-following.

Based on the above assumption and principle, the equation of MSS is shown as

$$
\begin{aligned}
d_{mrdh} &= \begin{cases} \max\left(d'_{mrdh}, \tau_{rd} v_{rd}\right), & \text{if } (v_{rd} - v_h) \geq -5/3.6 \\ \tau_{rd} v_{rd}, & \text{if } (v_{rd} - v_h) < -5/3.6 \end{cases} \\
d_{mldh} &= \max\left(\tau_{ld} v_h - \frac{v_h^2}{2a_{\max}} + \frac{v_{ld}^2}{2a_{\max}}, \tau_{ld} v_h\right) \\
d_{mroh} &= \tau_{ro} v_{ro} \\
d_{mloh} &= \tau_{lo} v_h \\
d'_{mrdh} &= \tau_{re}(v_{rd} - v_h) - \frac{(v_{rd} - v_h)^2}{2a_{rd}} + \tau_{rd} v_h.
\end{aligned} \tag{1}
$$

In (1), $d_{mrdh}, d_{mldh}, d_{mroh}, d_{mloh}$ are the MSS between H and each surrounding vehicle, τ_{re} is the reaction time including driver reaction time and brake system response time, τ_{rd}, τ_{ld}, τ_{ro}, τ_{lo} are the safe THW between H and each surrounding vehicle, $\nu_{rd}, \nu_{ld}, \nu_{ro}, \nu_{lo}$ are the speeds of the surrounding vehicle, ν_h is the speed of vehicle H, a_{rd} is the brake acceleration of R_d, and $a_{\max}$ is the maximum brake acceleration.

It should be noted that the driving style varies for different drivers. Aggressive drivers tend to change lanes using short intervehicle distances, whereas conservative drivers may require a longer distance. The driving style factor c_{style} was adopted to adjust the MSS, causing the warning time to satisfy the individual driver's risk awareness. The value of c_{style} is set by the driver. If the value of c_{style} is greater than 1, it means that the driver is conservative, whereas a lesser value means that the driver is aggressive. The modified MSS is

$$
\begin{aligned}
d_{crdh} &= c_{\text{style}} d_{mrdh} \quad d_{cldh} = c_{\text{style}} d_{mldh} \\
d_{cloh} &= c_{\text{style}} d_{mloh} \quad d_{croh} = c_{\text{style}} d_{mroh}.
\end{aligned} \tag{2}
$$

In (2), $d_{crdh}, d_{cldh}, d_{croh}, d_{cloh}$ are the modified MSS of an individual driver.

IV. LCACC Controller Algorithm

The controller algorithm is designed on the basis of the MPC theory framework. The algorithm first builds vehicle and intervehicle dynamic models, which mainly contain the dynamic model of H, the dynamic models of the surrounding vehicles, and the driver's desired car-following model. Then, it constructs the comprehensive performance index for a single sample period, including the three subperformances of tracking, safety, and comfort. Finally, it derives all of the state variables in the predictive horizon, solves the optimization problem, and obtains the desired longitudinal acceleration.

A. Dynamic Model

With the exception of the control of longitudinal dynamic movement, LCACC also needs to consider spatial relationships between vehicle H and each surrounding vehicle. Thus, dynamic models contain the longitudinal dynamic models of H and the four surrounding vehicles, as well as the driver's desired car-following model.

When designing the longitudinal dynamic model of H, the mathematical relationship between the actual longitudinal acceleration and the desired longitudinal acceleration is described by

$$a_x = \frac{K_g}{T_g s + 1} a_{x\,\mathrm{des}}. \tag{3}$$

In (3), a_x is the actual longitudinal acceleration, K_g is the system gain, and T_g is the time constant [11].

Combining (3) with the vehicle's longitudinal kinematics, the longitudinal dynamic model of H is given by

$$\begin{aligned} \dot{\boldsymbol{x}}_h &= \boldsymbol{A}_{\mathrm{cont}} \boldsymbol{x}_h + \boldsymbol{B}_{\mathrm{cont}} u \\ \boldsymbol{A}_{\mathrm{cont}} &= \begin{bmatrix} 0 & 1 & T \\ 0 & 0 & 1 \\ 0 & 0 & -1/T_g \end{bmatrix} \\ \boldsymbol{B}_{\mathrm{cont}} &= \begin{bmatrix} 0 \\ 0 \\ K_g/T_g \end{bmatrix}. \end{aligned} \tag{4}$$

In (4), $\boldsymbol{x}_h = [s_h, v_h, a_h]^{\mathrm{T}}$ is the state variable, $\mathrm{u} = a_{x\,\mathrm{des}}$ is the system input, $\boldsymbol{A}_{\mathrm{cont}}$ is the state matrix, $\boldsymbol{B}_{\mathrm{cont}}$ is the input to state matrix, and T is the sampling time. Finally, a constant period sample and a zero-order holder are used in the data processing of the controller.

To simply the algorithm, assume that during the prediction horizon, the surrounding vehicles drive with constant longitudinal acceleration during the current sample time and the longitudinal dynamic models of the surrounding vehicles are described by

$$\begin{aligned} \boldsymbol{x}_{sv}(k+1|k) &= \boldsymbol{A}_{sv} \boldsymbol{x}_{sv}(k) \\ \boldsymbol{A}_{sv} &= \begin{bmatrix} 1 & T & T^2/2 \\ 0 & 1 & T \\ 0 & 0 & 1 \end{bmatrix} \\ sv &\in (lo, ld, ro, rd). \end{aligned} \tag{5}$$

In (5), $\boldsymbol{x}_{sv} = [s_{sv}, v_{sv}, a_{sv}]\mathrm{T}$ is the state variable, and $\boldsymbol{A}_{sv}$ is the state matrix.

The desired car-following distance is described by

$$d_{\mathrm{des}} = \tau \cdot v_h + d_{\mathrm{safe}}. \tag{6}$$

In (6), d_{des} is the desired distance, τ is the desired time constant, and d_{safe} is the safe stopping distance.

Meanwhile, assume that in the predictive horizon, vehicle H also drives at a constant longitudinal acceleration in the current sample time. The desired car-following distance in the predictive horizon is given by

$$\begin{aligned} d_{\mathrm{des}}(k+1|k) &= \boldsymbol{A}_{\mathrm{des}}(k+1|k) x_{sv}(k) + B_{\mathrm{des}} \\ \boldsymbol{A}_{\mathrm{des}}(k+1|k) &= [0 \quad \tau \quad \tau T] \\ B_{\mathrm{des}} &= [d_{\mathrm{safe}} \quad d_{\mathrm{safe}} \quad d_{\mathrm{safe}}]^T. \end{aligned} \tag{7}$$

In (7), $\boldsymbol{A}_{\mathrm{des}}$ and B_{des} are the coefficient matrices.

Then, the distance error and relative speed are used to describe the intervehicle dynamic characteristics as

$$\begin{aligned} \Delta d_{lh}(k+1|k) &= d_{lh}(k+1|k) - d_{\mathrm{des}}(k+1|k) \\ d_{lh}(k+1|k) &= s_l(k+1|k) - s_h(k+1|k) \\ \Delta v_{lh}(k+1|k) &= v_h(k+1|k) - v_l(k+1|k). \end{aligned} \tag{8}$$

In (8), Δd_{lh} is the distance error between H and the leading vehicle, d_{lh} is the distance between the two vehicles, s_l is the longitudinal position of the leading vehicle, s_h is the longitudinal position of H, Δv_{lh} is the relative speed of H and the leading vehicle, and v_l is the speed of the leading vehicle. Here, the leading vehicles are L_o and L_d.

B. Design of Tracking Performance Index

The main objective of LCACC's tracking performance is to smoothly switch the leading vehicle from L_o before lane change to L_d after lane change. For the sake of the "smoothly switch," we assume the two leading vehicles as a virtual leading vehicle and refer to the algorithm of conventional ACC to design the tracking performance of LCACC.

The objectives of conventional ACC are as follows: 1) When the preceding vehicle drives steadily, the distance error and relative speed should converge to 0. 2) When the preceding vehicle accelerates or brakes, the distance error and relative speed change within the driver's desired error range, preventing the occurrence of sudden cut-in due to a large intervehicle distance or unexceptional rear collisions due to a small distance. For the former object, the 2-norm of the distance error and relative speed is used as the cost function of the tracking performance index. For the latter, the 1-D distribution model of the driver's desired tracking error is adopted as the constraint of the tracking performance index.

LCACC's tracking performance is mainly reflected as follows: There are two tracking target vehicles, and the target gradually transforms from L_o to L_d. First, H is located in the center of the originating lane, so the target is solely L_o. When crossing

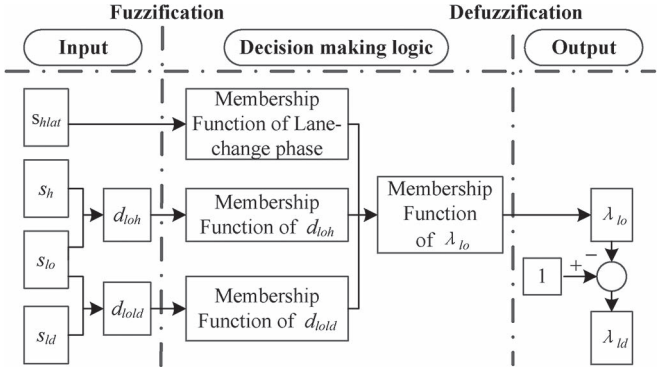

Fig. 2. Fuzzy logic car-following weights' conditioning system.

the lane mark, H needs to try to follow L_d while avoiding a collision with L_o; hence, it should follow the two leading vehicles simultaneously. After successfully crossing the lane mark, V_h will neglect L_o and just follow L_d instead. Based on this, tracking performance should be coordinated between the two target vehicles; hence, the cost function is separately designed as the linear weighted results of the tracking performances between H and the two leading vehicles. The constraint remains the same as that of the conventional ACC.

The designed tracking performance cost function of LCACC is shown by

$$L_{\mathrm{tra}} = \lambda_{lo}\left(w_{\Delta d}\Delta d_{loh}^2 + w_{\Delta v}\Delta v_{loh}^2\right) + \lambda_{ld}\left(w_{\Delta d}\Delta d_{ldh}^2 + w_{\Delta v}\Delta v_{ldz}^2\right). \quad (9)$$

In (9), L_{tra} is the quadratic index, λ_{lo} and λ_{ld} are the car-following weights between H and the two leading vehicles, Δd_{loh} and Δd_{ldh} are the distance errors, Δv_{loh} and Δv_{ldh} are relative speeds, $\omega_{\Delta d}$ is the weight of the distance error, and $\omega_{\Delta v}$ is the weight of the relative speed.

The constraints of tracking performance are

$$\begin{aligned} \Delta d_{\min}\cdot S_{\mathrm{DE}}^{-1} \le \Delta d \le \Delta d_{\max}\cdot S_{\mathrm{DE}}^{-1} \\ \Delta v_{\min}\cdot S_{\mathrm{VE}}^{-1} \le \Delta v \le \Delta v_{\max}\cdot S_{\mathrm{VE}}^{-1}. \end{aligned} \quad (10)$$

In (10), $\Delta d_{\min}$ and $\Delta d_{\max}$ are the limits of the distance error, $\Delta v_{\min}$ and $\Delta v_{\max}$ are the limits of the relative speed, and S_{DE} and S_{VE} are the driver's sensitivity to the distance error and relative speed, respectively.

Because changes to the relative positions between H and the two leading vehicles are timely during the lane-change process, setting suitable car-following weights is key to realizing smooth switching between the two targets. In a real driving environment, the driver defines the lane-change phases by checking the lateral position of H and assesses the priority target vehicle by observing the three vehicles' longitudinal positions. Finally, he/she adjusts the longitudinal speed of H. All of the perception to information is considered to be qualitative judgment. Here, the fuzzy logic method is adopted to simulate the driver's decision-making process, and the car-following weights' conditioning system is shown in Fig. 2. Table I shows the fuzzy rules. The fuzzification method is minimum algorithm, and the defuzzifacation is solved by the weighted average method.

In Table I, the lane-change process is divided into four phases, including start lane change, before crossing lane line, after crossing lane line, and finish lane change. The longitudinal intervehicle distance between L_o and H includes three conditions: near, medium, and far. The longitudinal special relationship between L_o and L_d is classified as behind, close, and ahead. The weight values are defined as having seven grades, which are very small, small, medium small, medium, medium big, big, and very big.

TABLE I
FUZZY RULES

Distance between Lo and H	Distance between Lo and Ld	Lane-change phase			
		Start	Before-C	After-C	Finish
Near	Ahead	MB	M	S	VS
	Close	B	M	S	VS
	Behind	VB	M	S	VS
Medium	Ahead	MS	MS	S	VS
	Close	M	MS	S	VS
	Behind	MB	MS	S	VS
Far	Ahead	VS	VS	VS	VS
	Close	S	S	VS	VS
	Behind	MS	S	VS	VS

C. Safety Performance Index Design

Two main methods are employed to design the safe intervehicle distance. These are to 1) maintain steady car-following and to 2) avoid collisions. For the former, the distance that is larger than a certain safe value is called the safe intervehicle distance. However, this is available only under the steady following condition. Because the intervehicle distances of H and the surrounding vehicles vary throughout the entire lane-change process, this method is too simple to satisfy the safety requirement. For the latter, TTC and the relative speed are adopted to describe the safe intervehicle distance. However, this method is suitable only under the CA situation instead of steady following. By combining the two methods, the safety performance index is designed as in

$$\begin{aligned} d_{sloh} &\ge \max\left(\tau_{\mathrm{THW}lo}v_h, \tau_{\mathrm{TTC}lo}(v_h - v_{lo})\right) \\ d_{sldh} &\ge \max\left(\tau_{\mathrm{THW}ld}v_h, \tau_{\mathrm{TTC}ld}(v_h - v_{ld})\right) \\ d_{sroh} &\ge \max\left(\tau_{\mathrm{THW}ro}v_{ro}, \tau_{\mathrm{TTC}ro}(v_{ro} - v_h)\right) \\ d_{srdh} &\ge \max\left(\tau_{\mathrm{THW}rd}v_{rd}, \tau_{\mathrm{TTC}rd}(v_{rd} - v_h)\right). \end{aligned} \quad (11)$$

In (11), $d_{sloh}, d_{sldh}, d_{sroh}, d_{srdh}$ are the safe car-following distances, $\tau_{\mathrm{THW}lo}, \tau_{\mathrm{THW}ld}, \tau_{\mathrm{THW}ro}, \tau_{\mathrm{THW}rd}$ are the safe THW, and $\tau_{\mathrm{TTC}l}, \tau_{\mathrm{TTC}ld}, \tau_{\mathrm{TTC}ro}, \tau_{\mathrm{TTC}rd}$ are the safe TTC.

There are four car-following systems in the lane-change process, and the safety levels vary for each of them; hence, the parameter design for the four systems should be different. If there is a risk during car-following, the driver will brake to escape collision; thus, research on drivers' brake characteristics will support parameter design. For the car-following system on a highway, the reasons for rear vehicle braking are reflected mainly in three aspects: Response to Leading Vehicle Brake (RLVB), Cutting in (Cut-in), and Catching up Slower Vehicle Ahead (CSVA). Generally, a potential reason for braking between H and L_d is due to RLVB, a potential reason for

TABLE II
PARAMETER DESIGN FOR SAFETY PERFORMANCE

Brake Vehicle	Leading Vehicle	Brake Reason	THW (s)	TTC (s)
V_h	V_{ld}	RLVB	1.4	8.2
V_h	V_{lo}	CSVA	1.4	8.4
V_{rd}	V_h	Cut-in	1.8	10.5
V_{ro}	V_h	Cut-in	1.8	10.5

braking between H and L_o is due to CSVA, and the reason for braking between H and L_d is Cut-in; if lane change is canceled, H belongs to the "Cut-in" vehicle to R_o. We carried out field experiments on a highway with 12 participants, extracted THW and TTC values under the three brake reasons for each driver, and calculated the 50% cumulative frequency value, which reflected the driver's normal driving behavior. For "RLVB," the average and standard deviation values of all the participants are 1.39/0.29 s for THW and 8.24/1.63 s for TTC. For "CSVA," the average and standard deviation values are 1.41/0.29 s for THW and 8.41/1.62 s for TTC. For "Cut-in," the average and standard deviation values are 1.78/0.39 s for THW and 10.67/2.12 s for TTC. To simplify the algorithm, we ignored the driving differences and referred the average to design the parameter of safety performance as Table II shows.

D. Comfort Performance Index Design

The effectiveness of the LCACC system not only requires support from objective data but also needs the driver's subjective evaluation. Hence, with the exception of tracking and safety, the LCACC system should also satisfy the driver's longitudinal ride comfort request. Here, the longitudinal comfort performance index is mainly reflected in the fact that 1) the tracking errors fall within the driver's desired range, avoiding forward collisions or cutting in; 2) the vehicle should maintain a constant speed as much as possible and reduce the frequency of accelerating or braking, which may cause feelings of discomfort; and 3) fluctuations in the acceleration should be within the driver's desired range and should prevent uncomfortable feelings caused by large acceleration or an emergency brake.

For the three conditions, the first condition is realized by tracking performance. When the relative speed is small and the distance error is close to 0, the first condition is naturally satisfied.

The second condition can be reached by limiting longitudinal acceleration and the jerk. To limit the parameter quantity in the cost function and reduce the uncertainty caused by the redundant weights, only acceleration is considered in the cost function as in (12). The jerk limit is realized by limiting the maximum difference of the desired accelerations between the current and the last sampling time, and the maximum difference is the product of maximum jerk and sampling time. Thus

$$L_{\mathrm{com}} = w_a a_{x\,\mathrm{des}}^2. \tag{12}$$

In (12), L_{com} is the quadratic index, and ω_a is the weight of the desired acceleration.

The third condition is realized by constraining the range of longitudinal acceleration. Hence, the constraint of the comfort performance index is given by

$$a_{\min} \le a_{x\,\mathrm{des}} \le a_{\max}. \tag{13}$$

In (13), $a_{\min}$ and $a_{\max}$ are the limits of the desired acceleration.

E. Optimization Problem

Based on the description above, the cost function and constraint for a sampling time are formulated as in

$$\begin{aligned} L_{\mathrm{index}} &= L_{\mathrm{tra}} + L_{\mathrm{com}} \\ &= \boldsymbol{x}_h^T \omega_{x2} \boldsymbol{x}_h + \omega_{x1} \boldsymbol{x}_h + \omega_a u^2 + c \end{aligned} \tag{14}$$

$$\begin{aligned} &\Delta d_{\min} \cdot S_{\mathrm{DE}}^{-1} \le \Delta d_{lh} \le \Delta d_{\max} \cdot S_{\mathrm{DE}}^{-1} \\ &\Delta v_{\min} \cdot S_{\mathrm{VE}}^{-1} \le \Delta v_{lh} \le \Delta v_{\max} \cdot S_{\mathrm{VE}}^{-1} \\ &d_{sah} \ge \max\left(\tau_{\mathrm{THW}} \cdot v_r, \tau_{\mathrm{TTC}} \cdot (v_r - v_l)\right) \\ &a_{\min} < a_{x\,\mathrm{des}} < a_{\max}. \end{aligned} \tag{15}$$

In (14), ω_{x1} and ω_{x2} are weights of the system state. In (15), d_{sah} is the safe car-following distance of the car-following system formed by H and each surrounding vehicle, and v_l and v_r are the leading vehicle and the rear vehicle separately.

The sampling time is 0.05 s, and the length of predictive horizon is 10. With the system states in the current sample time, we predict the states and derive the cost function and constraint in the prediction horizon, construct the optimization problem, transfer all of the polynomials to the forms related with the input vector in the prediction horizon, and the optimization problem in this paper is realized by

$$\begin{aligned} &\min J\left(x_h(k), \boldsymbol{U}\right) \\ &\text{Subject to}: \quad \boldsymbol{A}_U \boldsymbol{U} \le \boldsymbol{b}_U. \end{aligned} \tag{16}$$

In (16), J is the cost function, $\boldsymbol{U}$ is the input vector in the prediction horizon, and $\boldsymbol{A}_U$ and $\boldsymbol{b}_U$ are the coefficient matrix and constant in the inequality. The cost function is given as

$$\begin{aligned} J &= \sum_{i=1}^{P} \Big(\|\boldsymbol{x}_h(k+i|k)\|^2_{\omega_{x2}(k+\mathrm{i}|k)} + \omega_{x1}(k+i|k)\boldsymbol{x}_h(k+i|k) \\ &\qquad + \|u(k+i|k)\|^2_{\omega_a} + c(k+i|k) \Big) \\ &= \boldsymbol{X}_h^T \boldsymbol{W}_{X2} \boldsymbol{X}_h + \boldsymbol{W}_{X1} X_h + \boldsymbol{U}^T \boldsymbol{R} \boldsymbol{U} + c \\ &= \left(\boldsymbol{A}_P \boldsymbol{x}_h(k) + \boldsymbol{B}_P \boldsymbol{U}\right)^T \boldsymbol{W}_{X2} \left(\boldsymbol{A}_P \boldsymbol{x}_h(k) + \boldsymbol{B}_P \boldsymbol{U}\right) \\ &\quad + \boldsymbol{W}_{X1} \left(\boldsymbol{A}_P \boldsymbol{x}_h(k) + \boldsymbol{B}_P \boldsymbol{U}\right) + \boldsymbol{U}^T \boldsymbol{R} \boldsymbol{U} + c \\ &= \frac{1}{2} \boldsymbol{U}^T \boldsymbol{H} \boldsymbol{U} + \boldsymbol{f}^T \boldsymbol{U} + c. \end{aligned} \tag{17}$$

In (17), $\boldsymbol{X}_h$ is the system state in the prediction horizon, $\boldsymbol{W}_{x2}$ and $\boldsymbol{W}_{x1}$ are the coefficient matrices of $\boldsymbol{X}_h$, $\boldsymbol{R}$ is the coefficient matrix of $\boldsymbol{U}$, $\boldsymbol{X}_h = \boldsymbol{A}_P x_h(k) + \boldsymbol{B}_P \boldsymbol{U}$, and $\boldsymbol{A}_P$ and $\boldsymbol{B}_P$ are the coefficient matrices in the state function. The cost function is finally formed as the dependent variable of $\boldsymbol{U}$, and $\boldsymbol{H}$ and $\boldsymbol{f}$ are the coefficient matrices of $\boldsymbol{U}$ in the final form.

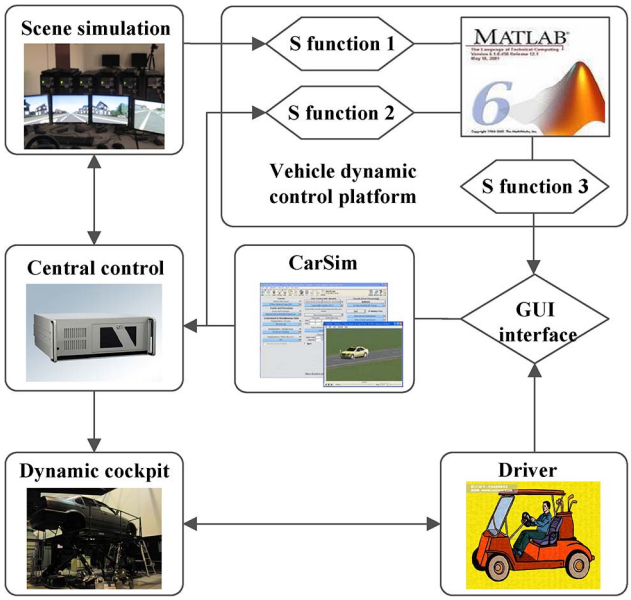

Fig. 3. Driving simulator structure.

The coefficient matrices in (16) are

$$\boldsymbol{A}_U = \begin{bmatrix} \boldsymbol{A}_{chp} \\ \boldsymbol{A}_{ci} \end{bmatrix}, \quad \boldsymbol{b}_U = \begin{bmatrix} \boldsymbol{b}_{chp} \\ \boldsymbol{b}_{ci} \end{bmatrix}$$

$$\boldsymbol{A}_{chp} = \boldsymbol{A}_{ch}\boldsymbol{A}_p, \quad \boldsymbol{b}_{chp} = \boldsymbol{b}_{ch} - \boldsymbol{A}_{ch}\boldsymbol{A}_p\boldsymbol{x}_h(k)$$

$$\boldsymbol{A}_{ch} = \begin{bmatrix} \boldsymbol{A}_c & & \\ & \ddots & \\ & & \boldsymbol{A} \end{bmatrix}, \quad \boldsymbol{b}_{ch} = \begin{bmatrix} \boldsymbol{b}_c(k+1|k) \\ \vdots \\ \boldsymbol{b}_c(k+P|k) \end{bmatrix}$$

$$\boldsymbol{A}_{ci} = \begin{bmatrix} 1 & & & \\ & \ddots & & \\ & & & 1 \\ -1 & & & \\ & \ddots & & \\ & & & -1 \end{bmatrix}, \quad \boldsymbol{b}_{ci} = \begin{bmatrix} u_{\max} \\ \vdots \\ u_{\max} \\ -u_{\min} \\ \vdots \\ -u_{\min} \end{bmatrix}$$

$$\boldsymbol{A}_c = \begin{bmatrix} 1 & 0 & 0 \\ -1 & 0 & 0 \\ 0 & 1 & 0 \\ 0 & -1 & 0 \end{bmatrix}, \quad \boldsymbol{b}_c(k+i|k) = \begin{bmatrix} \min(f_1, f_2, f_3) \\ \min(f_4, f_5, f_6) \\ f_7 \\ f_8. \end{bmatrix} \tag{18}$$

In (18), $\boldsymbol{A}_{chp}$ and $\boldsymbol{b}_{chp}$ are the coefficient matrix and constant matrix of the inequality formed by the first three inequalities of (15) in the prediction horizon, and $\boldsymbol{A}_{ci}$ and $\boldsymbol{b}_{ci}$ are the coefficient matrix and constant matrix of the inequality formed by the last inequality of (15) in the prediction horizon.

We soften the hard constraints by adopting a constraint management method, and we extend the algorithm's feasible region. Using the Dantzig–Wolfe method to solve the proposed optimization problem [22], we eventually obtain the desired longitudinal acceleration output using the LCACC controller.

V. Simulation and Analysis

To verify the effect of the LCACC system, the simulation experiment was completed on the driving simulator under two scenarios and was compared with conventional ACC. As Fig. 3 shows, in the driving simulator, the vehicular dynamic software Carsim was used to simulate the output of dynamic movement, and the controller was constructed using MATLAB/Simulink. To confirm the effectiveness of the comparison, the conventional ACC controller was designed according to the LCACC algorithm: The two car-following weights 1) no longer change continuously from 0 to 1, but change to 0 or 1 instead, 2) cancel the safety performance index of LCACC, and 3) cause the other parameters to remain unchanged. Of the two scenarios, the first involves the scenario where there are two leading vehicles. This is to verify tracking performance. The second scenario is the L_o emergency brake scenario, which is to verify safety performance.

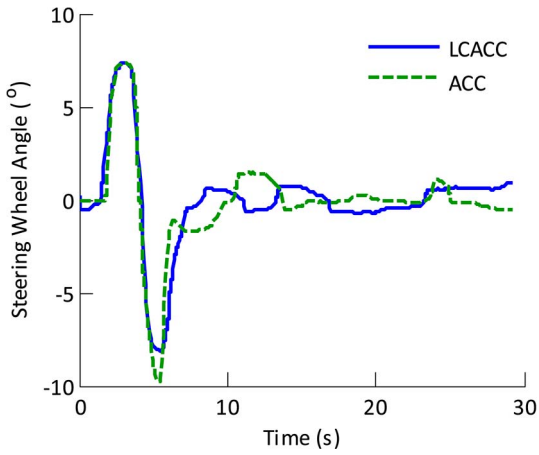

Fig. 4. Steering wheel angle for S1.

A. Scenario Involving Two Leading Vehicles

In this scenario (S1), H first cruises at 80 km/h, whereas L_o is 40 m behind H. L_d is 30 m ahead of L_o, and both R_o and R_d are 30 m behind L_o; all of the surrounding vehicles drive at the same speed as H. Then, the speed of L_o changes to 70 km/h, and the speeds of the other three vehicles change to 75 km/h. When the driver realizes that the speed of L_o is reduced, he begins to change lane. The data are obtained during a certain period for analysis, from the moment when L_o changes to 70 km/h to the moment 30 s after.

Fig. 4 indicates the curves of the steering wheel angle, Fig. 5 shows the curves of longitudinal acceleration, Fig. 6 presents the curves of longitudinal speed, and Fig. 7 shows the curves of the tracking parameters between H and L_d with the two systems.

Fig. 4 shows that the lane-change moments and the steering wheel angles are similar to each other with the two systems, and this ensures that the simulation results with the two systems are comparable.

In Fig. 5, H decelerates to respond to the speed change of L_o first, and then, the driver begins to change lane. Since the speed of L_d is higher than L_o, H accelerates again to follow L_d. In the acceleration phase, the adjustment moment is earlier, and the adjustment duration is about 3 s shorter with the LCACC system. Meanwhile, the maximum acceleration is 0.4 m/s^2 with the LCACC system and 0.9 m/s^2 with the ACC system. This consequently indicates the better comfort performance of LCACC.

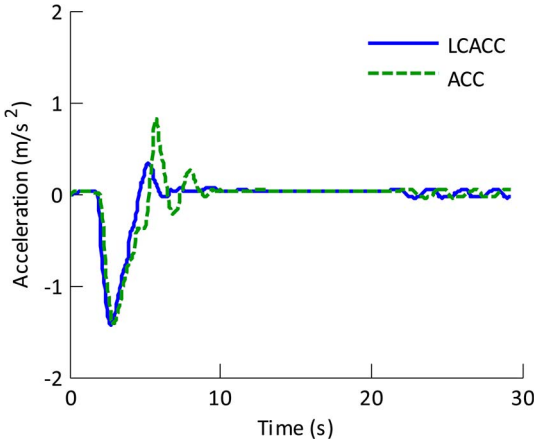

Fig. 5. Longitudinal acceleration for S1.

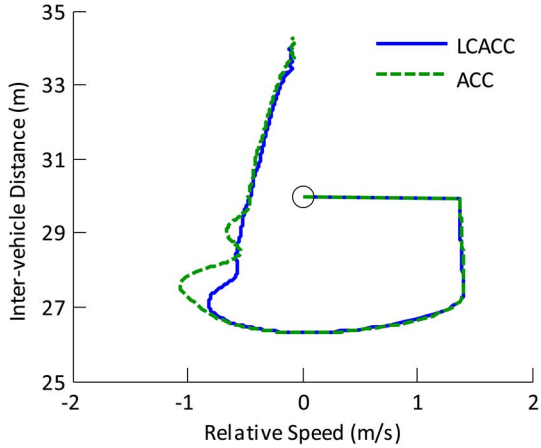

Fig. 7. Tracking parameter for S1.

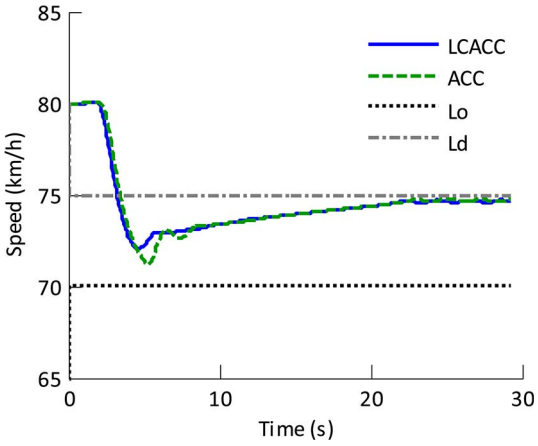

Fig. 6. Longitudinal speed for S1.

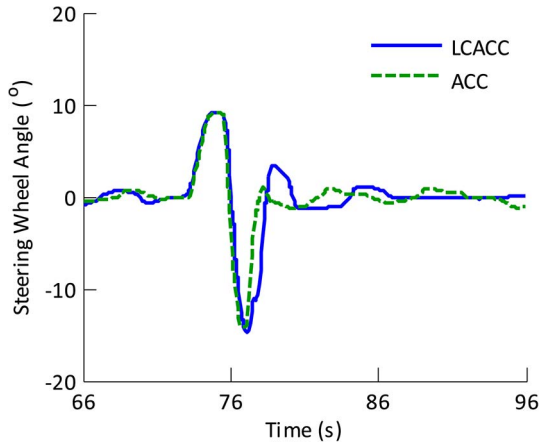

Fig. 8. Steering wheel angle for S2.

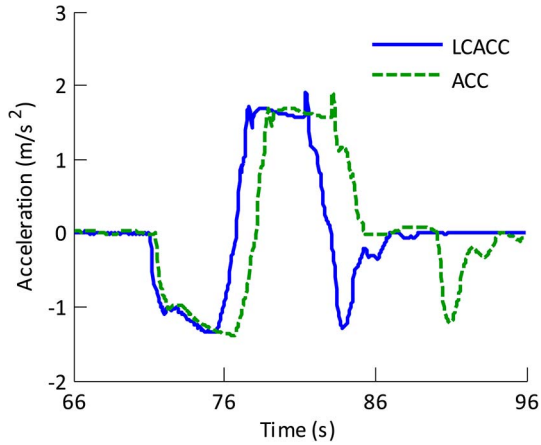

Fig. 9. Longitudinal acceleration for S2.

In Fig. 6, the speed trough with LCACC is about 1 km/h higher than the value with ACC, and the slope of the curve with LCACC is also smaller. Fig. 7 shows that the tracking parameters between H and L_d are more convergent with the LCACC system.

B. L_o Emergency Brake Scenario

In this scenario (S2), H first cruises at 90 km/h, with L_o being 35 m in front of H and L_d 1 m in front of H; both of the leading vehicles drive at 80 km/h, whereas the two rear vehicles are 40 m behind H and drive at 90 km/h. After 60 s, the speed of L_d changes to 85 km/h, the speed of R_o changes to 70 km/h, and the speed of R_d changes to 75 km/h. After another 10 s, L_o begins to brake with a deceleration of 1.5 m/s^2 for 10 s and then resumes uniform driving. When the driver detects that L_o has braked, he begins to change lane. For analysis, we extracted the data for the period from 10 s before the lane change and the moment 20 s after lane change.

Figs. 8–10 are the curves of the steering wheel angle, longitudinal acceleration, and speed with the two systems. Fig. 8 shows that the steering wheel angles are similar to those of the two systems. In Fig. 9, at the beginning of L_o's braking period, the accelerations of H are obviously affected for the two systems. When the driver begins to change lane, LCACC can adjust the acceleration in a timely manner and can minimize the braking influence of L_o. The moment at which LCACC begins to adjust the acceleration is 1.5 s earlier than with ACC. Meanwhile, the maximum deceleration with LCACC is smaller than the value with ACC.

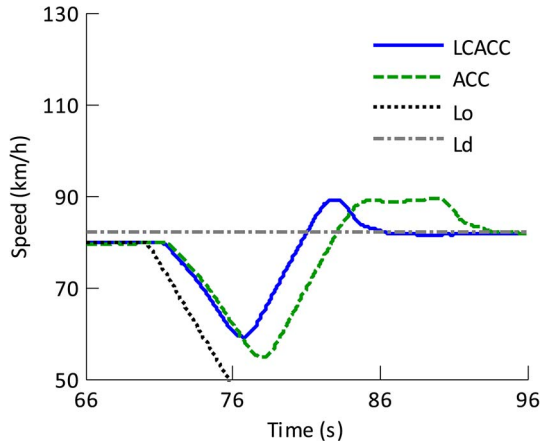

Fig. 10. Longitudinal speed for S2.

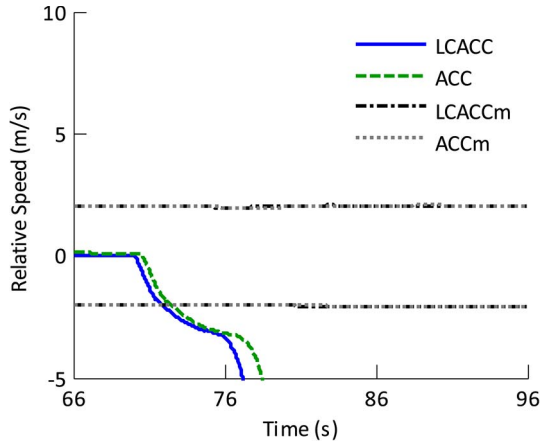

Fig. 11. Relative speed between H and L_o.

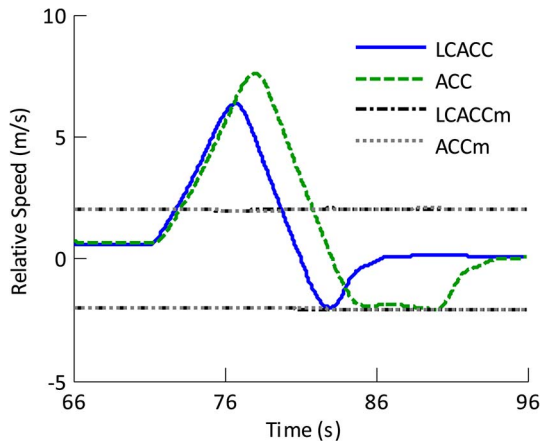

Fig. 12. Relative speed between H and L_d.

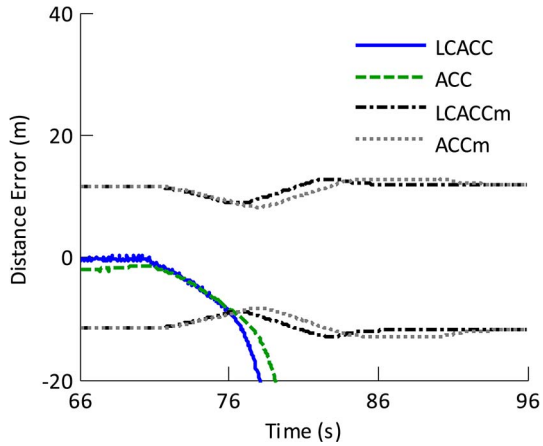

Fig. 13. Distance error between H and L_o.

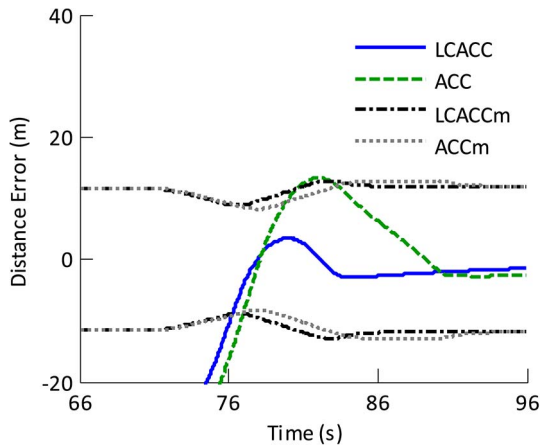

Fig. 14. Distance error between H and L_d.

In Fig. 10, H switches to the ACC mode after changing lane with the LCACC system; however, H first switches to the CC mode and then to the ACC mode after changing lane with the conventional ACC system. At the same time, the minimum speed is 58 km/h with the LCACC system and 55 km/h with the ACC system. Therefore, with LCACC, H is less affected by the braking of L_o.

Fig. 11 shows the relative speed between H and L_o. Fig. 12 shows the relative speed between H and L_d. Figs. 13 and 14 describe the distance error between H and the two leading vehicles. In Fig. 11, the relative speed is almost zero at first and then changes very quickly. The change moment with LCACC is about 1 s earlier than with ACC. In Fig. 12, during the adjusting process, the duration of the condition that the relative speed is out of the driver's desired range is 3 s shorter, the maximum of relative speed is 2 m/s smaller, and the moment when the value converges to 0 m/s is also 8 s earlier with the LCACC system. In Fig. 13, the distance error is almost zero at the beginning and then decreases quite quickly when L_o brakes. In Fig. 14, the moment when the distance error enters the driver's desired range is 1 s earlier with LCACC, and the moment when the value converges to 0 m is 8 s earlier, the maximum of the distance error is quite smaller than the limit of the driver's desired value with LCACC, whereas the value with ACC almost reaches the limit of the driver's desired value.

Figs. 15 and 16 show that the tracking parameters are more convergent with the LCACC system, whereas Figs. 15 and 16 indicate that the intervehicle distances between H and the two rear vehicles are larger than the safety car-following distance with the LCACC system and are smaller than the safe value with the ACC system. This is because the conventional ACC accelerates later and causes H to brake too much.

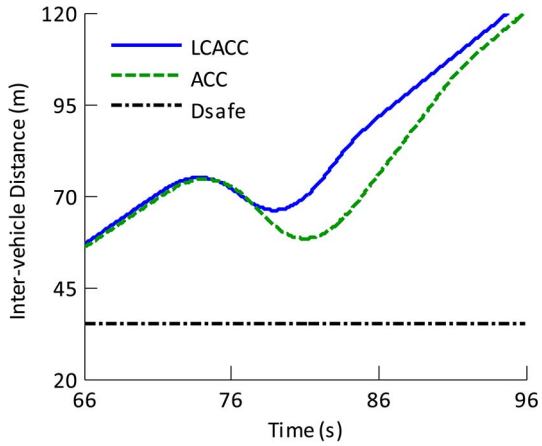

Fig. 15. Intervehicle distance between H and R_o.

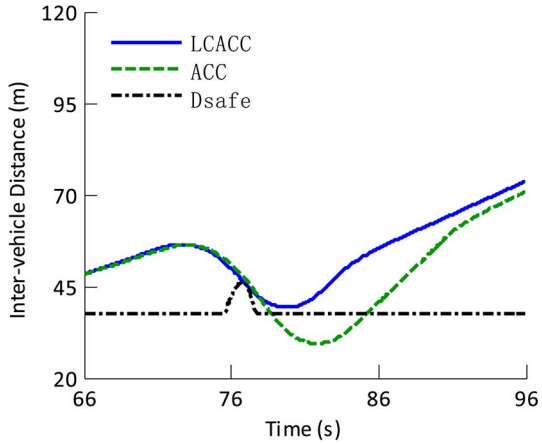

Fig. 16. Intervehicle distance between H and R_d.

VI. Conclusion

This paper has presented a coordinated LCACC. The system can monitor the risks associated with lane-change behavior considering the interaction with surrounding vehicles. The conclusions are listed as follows.

1) The proposed LCACC is able to address the issue where ACC may hinder lane-change behavior. The LCACC responds to the driver's lane-change intent, assesses the lane-change risk, and assists with the longitudinal movement of the host vehicle during lane change.
2) The lane-change warning algorithm considers the movement of surrounding vehicles and can achieve effective risk warning. The algorithm separately analyzes the MSS between the host vehicle and each surrounding vehicle, introducing the driver style factor to increase individual drivers' risk awareness.
3) The LCACC controller is designed on the basis of the MPC theory, which reaches multiobjective coordination optimization. The cost function is designed using the 2-norm number of the tracking error and desired acceleration, and the constraint of the input and output is described by linear inequality.
4) The driver-in-the-loop experiment performed in the driving simulator verifies the control effect of the LCACC system. The simulation results indicate that the proposed LCACC system can adjust the desired longitudinal acceleration to assist lane change and can realize multiobjective coordination.
5) A few additional explanations: Since the research work in this paper focuses on the design framework of LCACC, and we do not have mature conditions to complete the real vehicle experiment at present, the controller effect is verified in the driving simulator, the sensor and system uncertainties are considered as follows. The vehicle information is provided under the V2V communication, which already has processed the sensor uncertainties, and MPC is robust to system uncertainties. For the future real vehicle experiment, we will take sensor and system uncertainties into consideration.

References

[1] A. Vahidi and A. Eskandarian, "Research advances in intelligent collision and adaptive cruise control," *IEEE Trans. Intell. Transp. Syst.*, vol. 4, no. 3, pp. 143–153, Sep. 2003.
[2] S. E. Li, K. Li, and J. Wang, "Economy oriented vehicle adaptive cruise control with coordinating multiple objectives function," *Veh. Syst. Dyn.*, vol. 51, no. 1, pp. 1–17, Jan. 2013.
[3] D. Zhang, K. Li, and J. Wang, "A curving ACC system with coordination control of longitudinal car-following and lateral stability," *Veh. Syst. Dyn.*, vol. 50, no. 7, pp. 1085–1102, Jul. 2012.
[4] K. Li, T. Chen, Y. Luo, and J. Wang, "Intelligent environment-friendly vehicles: Concept and case studies," *IEEE Trans. Intell. Transp. Syst.*, vol. 13, no. 1, pp. 318–328, Mar. 2012.
[5] R. Bosch, "Adaptive Cruise Control," in *Safety, Comfort and Convenience Systems*, 3rd ed. Berlin, Germany: Federal Republic of Germany, 2004, pp. 193–194.
[6] C. M. Rudin-Brown and H. A. Parker, "Behavioural adaptation to Adaptive Cruise Control (ACC): Implications for preventive strategies," *Transp. Res. F, Traffic Psychol. Behav.*, vol. 7, no. 2, pp. 59–76, Mar. 2004.
[7] J. Freyer, B. Deml, M. Maurer, and B. Farber, "ACC with enhanced situation awareness to reduce behavior adaptations in lane change situations," in *Proc. IEEE Intell. Veh. Symp.*, Istanbul, Turkey, 2007, pp. 999–1004.
[8] D. Kim, S. Moon, J. Park, H. J. Kim, and K. Yi, "Design of an adaptive cruise control/collision avoidance with lane change support for vehicle autonomous driving," in *Proc. Int. Joint Conf. ICROS-SICE*, Fukuoka, Japan, 2009, pp. 2938–2943.
[9] L. Bageshwar, L. Garrard, and R. Rajamani, "Model predictive control of transitional maneuvers for adaptive cruise control vehicles," *IEEE Trans. Veh. Technol.*, vol. 53, no. 5, pp. 1573–1585, Sep. 2004.
[10] D. Corona and D. Schutter, "Adaptive cruise control for a SMART car: A comparison benchmark for MPC-PWA control methods," *IEEE Trans. Control Syst. Technol.*, vol 16, no. 2, pp. 365–372, Mar. 2008.
[11] S. E. Li, K. Li, R. Rajamani, and J. Wang, "Model predictive multiobjective vehicle adaptive cruise control," *IEEE Trans. Control Syst. Technol.*, vol. 19, no. 3, pp. 556–566, May 2011.
[12] M. Mukai and T. Kawabe, "Model predictive control for lane change decision assist system using hybrid system representation," in *Proc. Int. Joint Conf. SICE-ICASE*, Busan, Korea, 2006, pp. 5120–5125.
[13] H. Yoshida, S. Shinohara, and M. Nagai, "Lane change steering manoeuvre using model predictive control theory," *Veh. Syst. Dyn.*, vol 46, no. 1, pp. 669–681, Jan. 2008.
[14] P. Falcone, F. Borrelli, J. Asgari, S. E. Tseng, and D. Hrovat, "Predictive active steering control for autonomous vehicle systems," *IEEE Trans. Control Syst. Technol.*, vol. 15, no. 3, pp. 566–580, May 2007.
[15] P. Falcone, H. E. Tseng, F. Borrelli, J. Asgari, and D. Hrovat, "MPC-based yaw and lateral stabilization via active front steering and braking," *Veh. Syst. Dyn.*, vol. 46, no. S1, pp. 611–628, 2008.
[16] D. Limon *et al.*, "Input-to-state stability: A unifying framework for robust model predictive control," in *Nonlinear Model Predictive Control*. Berlin, Germany: Springer-Verlag, 2009, pp. 1–26.
[17] D. Q. Mayne, J. B. Rawlings, C. V. Rao, and P. O. M. Scokaert, "Constrained model predictive control: Stability and optimality," *Automatica*, vol. 36, no. 6, pp. 789–814, Jun. 2000.

[18] P. O. M. Scokaert, D. Q. Mayne, and J. B. Rawlings, "Suboptimal model predictive control (feasibility implies stability)," *IEEE Trans. Autom. Control*, vol. 44, no. 3, pp. 648–654, Mar. 1999.
[19] D. Lovett, "Improving MPC robustness using statistical process monitoring," in *Proc. UKACC Control*, Glasgow, U.K., Aug. 2006, pp. 75–85.
[20] P. Falugi and D. Q. Mayne, "Getting robustness against unstructured uncertainty: A tube-based MPC approach," *IEEE Trans. Autom. Control*, vol. 59, no. 5, pp. 1290–1295, May 2014.
[21] H. Li and Y. Shi, "Robust distributed model predictive control of constrained continuous-time nonlinear systems: A robustness constraint approach," *IEEE Trans. Autom. Control*, vol. 59, no. 6, pp. 1673–1678, Jun. 2014.
[22] R. Fletcher, *Practical Methods of Optimization*. Hoboken, NJ, USA: Wiley, 2000.

Ruina Dang received the B.Tech. and Ph.D. degrees from Tsinghua University, Beijing, China, in 2008 and 2014, respectively.

She is with China North Vehicle Research Institute, Beijing. Her research interests include driver-assistance systems and driver behavior and modeling.

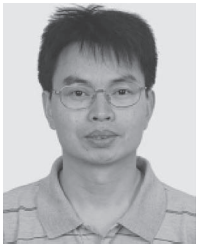

Jianqiang Wang received the B.Tech. and M.S. degrees from Jilin University of Technology, in 1994 and 1997, respectively, and the Ph.D. degree from Jilin University, Changchun, China, in 2002.

He is an Associate Professor of automotive engineering with Tsinghua University, Beijing, China. He has engaged in over ten projects such as the National Natural Science Foundation of China and the National High Technology Research and Development Program of China. He has authored over 40 journal papers and is a coinventor of 20 patent applications. His active research interests include intelligent vehicle, driving assistance systems, and driver behavior.

Dr. Wang has received six awards including the Jilin Province S&T Progress Award and the Chinese Automotive Industry S&T Progress Award.

Shengbo Eben Li received the M.S. and Ph.D. degrees from Tsinghua University, Beijing, China, in 2006 and 2009, respectively.

From 2010 to 2012, he was a Postdoctoral Researcher with University of Michigan, Ann Arbor, MI, USA. He is currently an Assistant Professor with the Department of Automotive Engineering, Tsinghua University. He has authored or coauthored more than 60 peer-reviewed journal/conference papers and holds more than ten patents. His active research interests include nonlinear dynamics and optimal control, autonomous vehicle, and control of battery.

Dr. Li received the Award for Science and Technology of China ITS Association (2012), the Award for Technological Invention in Ministry of Education (2012), the National Award for Technological Invention in China (2013), and the Honored Funding for Beijing Excellent Youth Researcher (2013).

Keqiang Li received the B.Tech. degree from Tsinghua University, Beijing, China, in 1985 and the M.S. and Ph.D. degrees from Chongqing University, Chongqing, China, in 1988 and 1995, respectively.

He is a Professor of automotive engineering with Tsinghua University. He has authored over 90 papers and is a coinventor of 12 patents in China and Japan. His main areas of research interest include vehicle dynamics and control for driver assistance systems and hybrid electrical vehicles.

Dr. Li is a Senior Member of the Society of Automotive Engineers of China and has served on the Editorial Board of *International Journal of ITS Research* and *International Journal of Vehicle Autonomous Systems*. He received the "Changjiang Scholar Program Professor" award and some awards from public agencies and academic institutions of China.